J. Physique **41** (1980) 87-96 JANVIER **1980**, PAGE 87

Classification
Physics Abstracts
64.70K — 61.12

The temperature dependence of the structures of $RbCaF_3$, and the determination of the low temperature phases

A. Bulou, C. Ridou, M. Rousseau, J. Nouet

Laboratoire de Physique de l'Etat Condensé, E.R.A. nº 682 (CNRS)
Faculté des Sciences, 72017 Le Mans Cedex, France

and

A. W. Hewat

Institut Laue-Langevin, 156 X Centre de Tri, 38042 Grenoble Cedex, France

(*Reçu le 18 juillet 1979, révisé le 25 septembre 1979, accepté le 27 septembre 1979*)

Résumé. — Nous reportons l'évolution en fonction de la température des paramètres structuraux (coordonnées et facteurs d'agitation thermique des ions) de part et d'autre de la transition de phase structurale cubique-quadratique dans $RbCaF_3$ à 193 K ainsi que la structure de ce composé au-dessous de 50 K. Ces études ont été réalisées par la méthode d'affinement du profil des raies de diffraction de neutrons sur poudre. Le même groupe d'espace ($Pnma\text{-}D_{2h}^{16}$) a été déterminé à 20 K et 4,5 K. L'égalité, à basse température, des angles de rotation des octaèdres CaF_6 autour de chacun des trois axes cubiques $\langle 100 \rangle$ ainsi que l'évolution des facteurs d'agitation thermique en phases cubique et quadratique permettent d'attribuer un caractère ordre-désordre aux transitions à 193 K et à 50 K.

Abstract. — The temperature dependence of the structural parameters (ions coordinates and ions temperature factors) in the vicinity of the cubic to tetragonal structural phase transition of $RbCaF_3$ at 193 K is reported together with the structure of this compound below 50 K. The neutron powder profile refinement method has been used to carry out this study. The same space group ($Pnma\text{-}D_{2h}^{16}$) has been found at 20 K and 4.5 K. Equality of the CaF_6 tilt angles about each of the three $\langle 100 \rangle$ cubic axes in the low temperature phase and the behaviour of the temperature factors in the cubic and tetragonal phases indicate an order-disorder character of the 193 K and 50 K phase transitions.

1. **Introduction.** — In the study of the phase transitions occurring in perovskite compounds ABX_3 and related to rotations of BX_6 octahedra, the tilt angles, which are assumed as the order parameters, are generally measured by indirect methods ; the more usual are EPR [1] and NMR [2]. However, in the first of these techniques, the paramagnetic probe disturbs the local surrounding (the most prosaic reason being the size difference of the intrinsic ion and the paramagnetic probe taking its place) and so can experience tilt angles different from the intrinsic ones. In the other technique, model have to be used to relate the measurements to the octahedron rotation angle, and more over, some parameters whose value is not known accurately have to be introduced. To explain the mechanism of these transitions, a model is put forward [3] which, to be confirmed, needs measurements of the absolute values of the tilt angles. Only a diffraction method is able to give these angles by the direct determination of ionic coordinates. The polydomain structure below the transition hinders the usual four circle diffraction technique and so, the Rietveld method (neutron powder profile refinement technique) [4, 5] seems to be the more convenient one [6]. Furthermore, when the transition is approached, some lattice modes go soft, which could, in theory [7], induce critical behaviour of the Debye-Waller factors of some ions [8] ; up to now, such a study against temperature has been done only in [9] under several assumptions or from indirect measurements of NMR relaxation time [10] which are closely related to these factors [7]. This Debye-Waller factors determination can be obtained by the Rietveld method modified by A. W. Hewat taking into account the anisotropy of these factors [5].

Transitions such as those discussed above are

encountered in $RbCaF_3$, in particular the 193 K ([1]) transition (O_h^1 to D_{4h}^{18}) [13, 14]. Moreover the additional presence of a central peak in the cubic phase [15] increases the interest of the Debye-Waller factor and tilt angle determination in this compound. It must be noted that this study could be even more fruitful in $RbCaF_3$ than in $SrTiO_3$ (similar transition at 105 K) in spite of the greater number of studies of the latter. The reason is that the larger distortion in $RbCaF_3$ should increase the tilt angle amplitude leading to better accuracy in the determination of its temperature dependence. Moreover, according to refs. [13] and [16] new phases appear at low temperature (phase transitions near 50 K and 7 K) whose structures are reported in this paper. The importance of the determination of these structures comes from the possibility to check different models forecasting them. This could also throw some light onto the mechanism of the 193 K phase transition.

The determination of the space groups of these phases can be carried out with the neutron powder profile refinement technique when used together with the Glazer classification of phases transition related to rigid tilts of octahedra in perovskite compounds [17].

2. **Data collection.** — Neutron diffraction measurements were performed on the D1A high resolution powder diffractometer on the high flux reactor at the ILL (Grenoble). This diffractometer has ten counters, with the counter bank sweeping through $2\theta = 6°$ to 160° in steps of 0.05° [18]. Wavelengths of 1.387 95(5) Å and 1.907 4(1) Å were used.

— The powder sample, inserted in a 16 mm vanadium can, was placed in a cryostat. The long term temperature stability was better than 0.5 K. Caution was taken in keeping the sample because of the hygroscopic character of the compound.

3. **Results.** — Measurements were performed at ten temperatures in the cubic and the tetragonal phases to get information about the thermal behaviour of both the atomic mean square displacement (B_{ij}) and the atomic coordinates. Two patterns were also recorded in each of the two lower temperature phases [16] to determine the new structures.

3.1 THE CUBIC TO TETRAGONAL PHASE TRANSITION. — The space groups O_h^1 (in the cubic phase) and D_{4h}^{18} (in the tetragonal phase) were assumed for the refinements. The tetragonal cell is shown figure 1 with the conventionnal pseudocubic subcell drawn inside. The atomic coordinates and the corresponding symmetry restriction on anisotropic temperature factor parameters are shown in table I*a* and I*b* for the cubic and tetragonal phase respectively. In the latter case u denotes the displacement from the special position of the ideal perovskite structure in fraction of

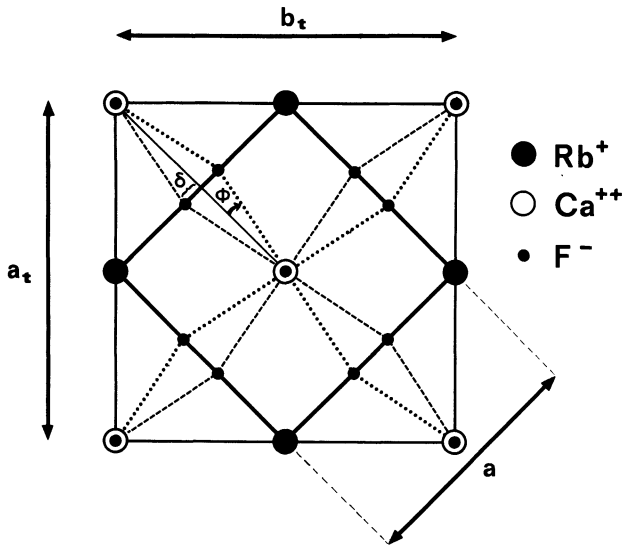

Fig. 1. — Projection in (001) plane of the tetragonal cell of $RbCaF_3$ with Ca at the origin. The dashed line shows the CaF bond at height 0 and the dotted line at the height 1/2 c_t. The projection of the conventionnal pseudocubic cell is drawn by a thick line.

Table I*a*. — $RbCaF_3$ *ions positions in the space group* O_h^1 *in the conventional cubic orientation and the corresponding symmetry restrictions on anisotropic temperature factors parameters (conventional cubic cell parameters* $a = b = c$*).*

		x	y	z	
Rb	1(b)	0.5	0.5	0.5	$B_{11} = B_{22} = B_{33}$
Ca	1(a)	0.	0.	0.	$B_{11} = B_{22} = B_{33}$
F	3(d)	0.	0.	0.5	$B_{11} = B_{22} \neq B_{33}$

Table I*b*. — *Fluorine displacements u from the cubic perovskite position in the space group* D_{4h}^{18} *in the conventional tetragonal orientation and the symmetry restrictions on anisotropic temperature factors parameters. The cell parameters are* a_t *and* c_t *related to the cubic ones according to* $a_t = a\sqrt{2}$ *and* $c_t = 2c$.

		x	y	z	
Rb	4(b)	0.	0.5	0.25	$B_{11} = B_{22} \neq B_{33}$
Ca	4(c)	0.	0.	0.	$B_{11} = B_{22} \neq B_{33}$
F	4(a)	0.	0.	0.25	$B_{11} = B_{22} \neq B_{33}$
F'	8(h)	0.25+u	0.75+u	0.	$B_{11} = B_{22} \neq B_{33} \neq B_{12}$

([1]) Several transition temperatures have been found from 193 K (powder diffraction studies) to 198 K (crystal studies). This effect has already been attributed by Kleeman [11] to the internal stress. The recent study of this compound under uniaxial stress by EPR [12] confirms this explanation.

Table II. — *Structural parameters in the cubic (a) and the tetragonal (b) phase of* $RbCaF_3$. *In each case*

$$R_{NUC} = 100\ \Sigma \mid I(\text{obs.}) - SI(\text{cal.}) \mid / \Sigma I(\text{obs.}),$$
$$R_{PROF} = 100\ \Sigma \mid Y_i(\text{obs.}) - SY_i(\text{cal.}) \mid / \Sigma Y_i(\text{obs.}),$$
$$R_{EXP} = 100\ \sqrt{(N-P)/\Sigma W \mid Y_i(\text{obs.}) \mid^2}, \quad \text{with} \quad I(\text{obs.}),\ I(\text{cal.})$$

integrated intensity of reflexion, Y_i (obs.), Y_i (cal.) *observed and calculated intensity data point, W weighting factor, N number of observations* Y_i, *P number of parameters, S scale factor. The* $B_{ij} = 8\pi^2 \overline{u_i u_j}$ *are given in* Å^2.

a)

T (K)	a_c (Å)	B_{11} (Rb)	B_{11} (Ca)	B_{11} (F)	B_{33} (F)	R_{NUC}	R_{PROF}	R_{EXP}
296	4.455 1(1)	1.86(2)	0.69(3)	3.63(3)	0.71(3)	1.37	6.92	2.74
250 (*)	4.451 8(1)	1.58(3)	0.62(3)	3.48(4)	0.42(4)	3.19	8.48	2.77
202	4.448 4(1)	1.37(2)	0.53(3)	3.30(3)	0.58(4)	1.41	6.70	2.52
199.7	4.448 4(1)	1.30(2)	0.54(3)	3.30(3)	0.56(3)	4.90	6.83	3.25

b)

T (K)	a_t	c_t	u	B_{11} (Rb)	B_{33} (Rb)	B_{11} (Ca)	B_{33} (Ca)	B_{11} (F)	B_{33} (F)	B_{11} (F')	B_{33} (F')	B_{12} (F')	R_{NUC}	R_{PROF}	R_{EXP}
186.5	6.286 1(1)	8.901 1(3)	0.016 0(2)	1.34(5)	1.07(9)	0.48(6)	0.55(11)	2.95(13)	0.58(10)	1.62(5)	3.00(12)	1.03(6)	1.69	6.54	3.03
170 (*)	6.280 5(1)	8.908 4(2)	0.021 6(2)	1.13(3)	1.23(6)	0.44(4)	0.60(7)	2.58(8)	0.69(7)	1.24(3)	2.65(7)	0.80(4)	5.36	9.43	3.40
150	6.274 4(1)	8.912 5(1)	0.025 2(1)	0.99(2)	1.08(4)	0.41(3)	0.45(5)	2.36(5)	0.52(4)	1.11(2)	2.35(4)	0.63(3)	1.78	6.10	3.18
120 (*)	6.267 2(1)	8.920 5(1)	0.029 5(1)	0.79(3)	0.86(4)	0.44(3)	0.49(5)	1.94(4)	0.52(4)	0.94(2)	1.92(4)	0.49(3)	3.80	7.50	3.23
87.5	6.259 1(1)	8.926 8(1)	0.032 7(1)	0.68(2)	0.71(3)	0.36(3)	0.33(4)	1.55(3)	0.44(3)	0.77(1)	1.50(3)	0.34(2)	2.03	5.92	3.21
55 (**)	6.251 7(1)	8.933 0(2)	0.035 2(2)	0.56(6)	0.76(9)	0.48(9)	0.42(12)	1.17(7)	0.93(1)	0.81(1)	1.37(7)	0.07(5)	3.32	8.00	2.14

(*) Measurements performed on an hydrated sample. The temperature factors (B_{ii}^h) deduced from the refinements are weaker than the absolute value and can be corrected according to $B_{ii} = B_{ii}^h + \Delta B$ where in this case $\Delta B = 0.30$.

(**) The bad value of the B_{ij} comes from the effect of a phase coexistence.

tetragonal cell parameter a_t (a_t, b_t, c_t are the tetragonal cell parameters). Tables II*a* and II*b* show the results of the refinements together with the reliability on them.

In order to show how these parameters behave at the transition, in the tetragonal phase we shall find it convenient to express them in the pseudocubic subcell. For simplicity the data will be refered to the axes chosen according to figure 2. We will denote a, b, and c the pseudocubic subcell parameters. They are related to the tetragonal cell parameters a_t, b_t and c_t according to

$$a = b = a_t/\sqrt{2} = b_t/\sqrt{2}, \quad c = c_t/2.$$

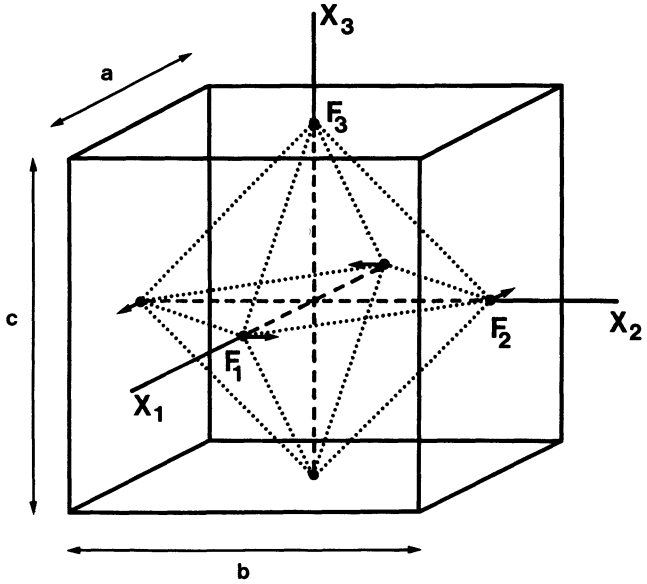

Fig. 2. — Conventional pseudocubic cell according to which the data will be noted. Arrows show the fluorine displacement occurring in the tetragonal phase.

The temperature dependence of pseudocubic cell parameters is shown figure 3.

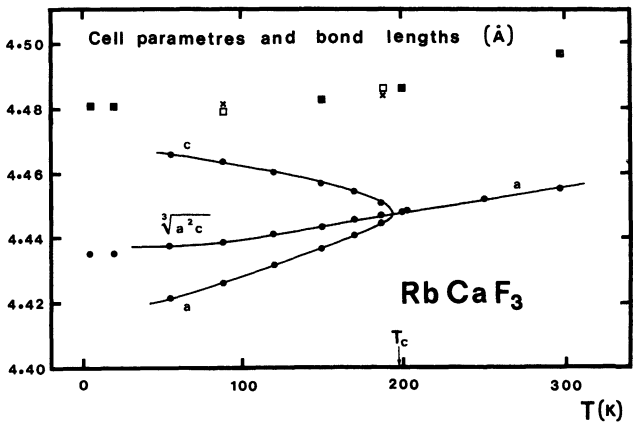

Fig. 3. — Temperature dependence of the pseudocubic cell parameters in cubic and tetragonal cells (full circles) and the temperature dependence of two times the CaF_1 (square) and CaF_3 (cross) bond lengths.

The F_1 displacement δ is related to the CaF_6 tilt angle φ by $\text{tg}\,\varphi = 2\,\delta/a$.

Figure 4 shows the temperature dependence of the tilt angle φ which is conventionally taken as the order parameter. The thermal behaviour of rubidium and calcium ions is plotted on figure 5, those of fluorine on figure 6. No absorption corrections have been made and so the absolute values of the temperature factors may be slightly greater.

These data allow to compute the CaF bond lengths. For this computation the very large thermal motion of fluorine must be taken into account [19]. When

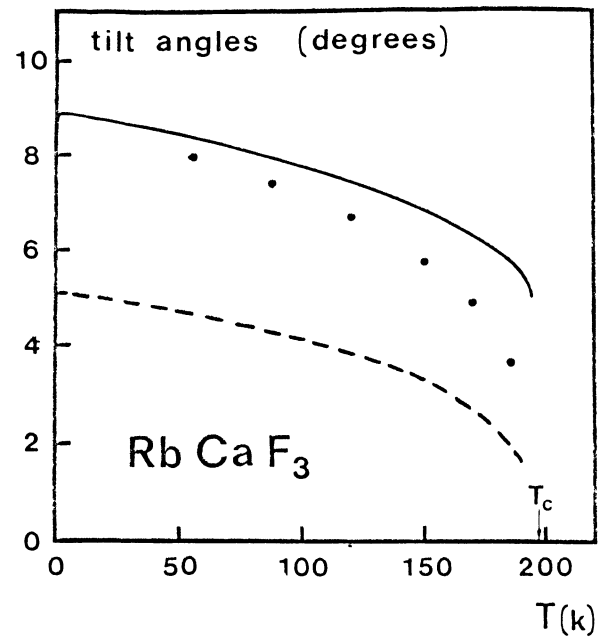

Fig. 4. — CaF_6 octahedron tilt angle according to the present result (full circles), the classical displacive model [26] (dashed line) and the order-disorder model [3] (solid line).

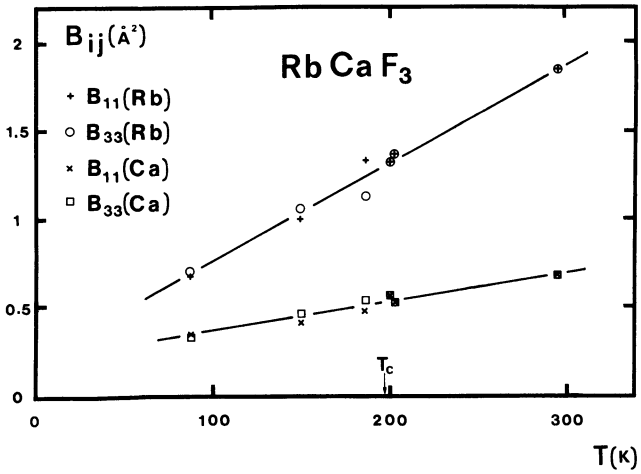

Fig. 5. — Thermal behaviour $B_{ii} = 8\pi^2 \bar{u}_i^2$ for rubidium and calcium ions according to the notations of figure 2.

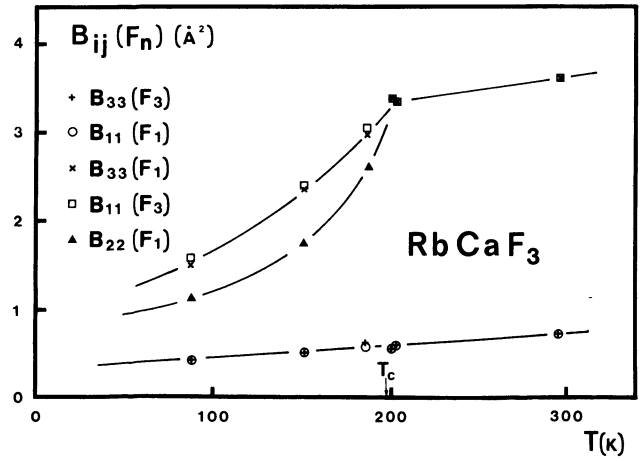

Fig. 6. — Thermal behaviour $B_{ii} = 8\pi^2 \bar{u}_i^2$ for fluorines according to the notations of figure 2.

denoting l_a and l_c the instantaneous values of CaF_1 and CaF_3 bond lengths respectively one can write :

$$\frac{a}{2} = \frac{l_a}{2} \cos \varphi_2(F_1) \cos \varphi_3(F_1) \quad (1)$$

$$\frac{c}{2} = \frac{l_c}{2} \cos \varphi_1(F_3) \cos \varphi_2(F_3) \quad (2)$$

where φ_i refers to the tilt angle about X_i axis (including both static and dynamic effects). The measured data are the mean values (denoted by a bar) and so :

$$\bar{l}_a \simeq a\left(1 + \frac{\overline{\varphi_3^2(F_1)}}{2} + \frac{\overline{\varphi_2^2(F_1)}}{2}\right) \quad (3)$$

$$\bar{l}_c \simeq c\left(1 + \frac{\overline{\varphi_1^2(F_3)}}{2} + \frac{\overline{\varphi_2^2(F_3)}}{2}\right) \quad (4)$$

where it has been assumed weak values of φ_i. Now

$$\varphi_i(F_j) = \overline{\varphi_i(F_j)} + \Delta\varphi_i(F_j)$$

and $\overline{\varphi_i(F_j)} = 0$ apart from the tetragonal phase for $\varphi_3(F_1)$ which is equal to the order parameter φ (fig. 2). Replacing $\Delta\varphi_i(F_j)$ by the corresponding linear displacement $\bar{u}_i^2 = u_{ii} = \dfrac{B_{ii}}{8\pi^2}$ we are led to

$$(\bar{l}_a)^2 = a^2(1 + \varphi^2) + 4\,u_{22}(F_1) + 4\,u_{33}(F_1) \quad (5)$$

$$(\bar{l}_c)^2 = c^2 + 4\,u_{11}(F_3) + 4\,u_{22}(F_3)\,. \quad (6)$$

This correction for thermal librations is similar to the one proposed by Glazer [20]. The corrected CaF bond lengths $\bar{l}_a$ and $\bar{l}_c$ are reported in figure 3. All these data will be discussed in section 4.

3.2 THE STRUCTURE OF $RbCaF_3$ BELOW 50 K. — According to ref. [16], two phase transitions occur at $\sim$ 50 K and $\sim$ 7 K. A previous study [14] of some X-ray scattering lines (444, 622, 800 indexed in the double pseudocubic cell 2*a*, 2*b*, 2*c*) indicated clearly a phase coexistence (tetragonal plus unknown phase) in the temperature range 55 K to $\sim$ 10 K (fig. 7*a*). Below $\sim$ 10 K the disappearance of the tetragonal phase lines is observed without any modification of the unknown phase lines; so there is probably no phase transition at very low temperature; this is in agreement with the neutron powder diffraction experiment, the 20 K and 4.5 K patterns being quite similar.

A part of the neutron powder pattern recorded at 4.5 K is shown figure 8. Some of the lines are indexed in the double pseudocubic cell 2*a*, 2*b*, 2*c*. In addition to the main lines already present in the tetragonal phase (hkl all of the same parity) new lines are now present such as 310, 312, 314, 501, 512 (so-called M lines) and 320, 410, 421, 432, 520 (X lines). Assuming one of the Glazer space group [17] and according to its tilt system the presence of M lines indicates a (+) tilt. Moreover the X-ray study of the 444 reflexion

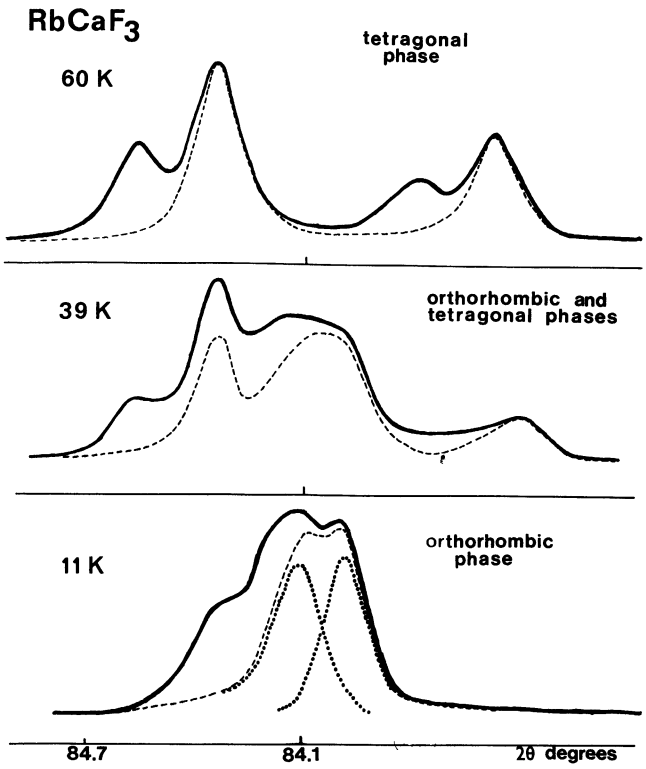

Fig. 7*a*. — X-ray diffraction powder study of the 622 line (according to 2*a*, 2*b*, 2*c*, pseudocubic cell) showing the phase coexistence. Measurements have been performed with the X-ray liquid helium cryostat [21] using the $K_{\alpha_1} - K_{\alpha_2}$ cobalt radiations

$$(\lambda_{K_{\alpha_1}} = 1.788\,92\ \text{Å})\,.$$

The dashed lines represent the patterns after removing the K_{α_2} radiation by the Rachinger method. The dotted line at 11 K shows the two components (622 and $\bar{6}22$) of the orthorhombic line.

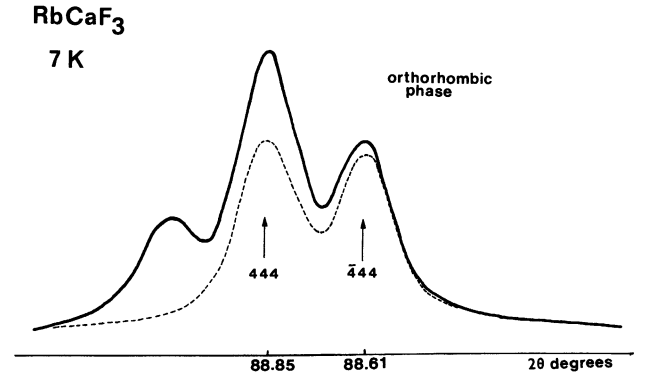

Fig. 7*b*. — Evidence of the splitting of the 444 line at 7 K recorded in the same conditions as in figure 7*a*.

showed that this line is split (fig. 7*b*), and so one of the double pseudocubic cell angles is different from 90°. Then only the $B2_1/m(11)$ and Pnma(62) space groups are allowed. The former is the more general of them and so refinements were carried out with it. The lattice parameters, atomic coordinates and the corresponding symmetry restriction on anisotropic temperature factor parameters are shown in table III.

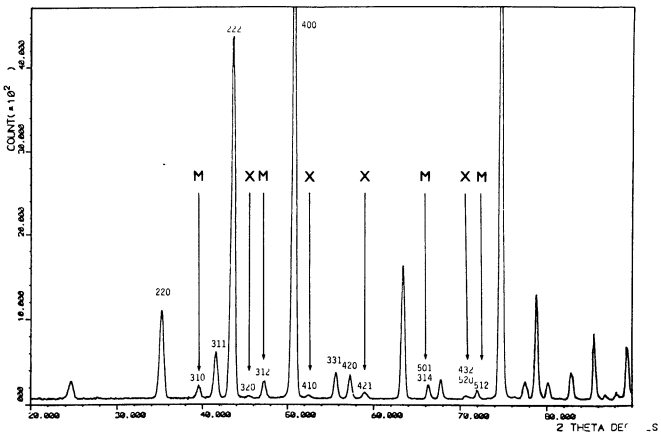

Fig. 8. — Part of the neutron diffraction powder pattern of $RbCaF_3$ at 4.5 K, showing the M and X superlattice lines. Vertical axis shows counts.

Table III. — *Displacements u, v, w from the cubic perovskite position in the space group* $B2_1/m$ *in the cell 2a, 2b, 2c and the corresponding symmetry restrictions on anisotropic temperature factors parameters.*

		x	y	z	B_{ij}
Rb_1	1(e)	$0.25+u_{R1}$	0.25	$0.25+w_{R1}$	$B_{11}\neq B_{22}\neq B_{33}\neq B_{31}$
Rb_2	1(e)	$0.25+u_{R2}$	0.25	$0.75+w_{R2}$	$B_{11}\neq B_{22}\neq B_{33}\neq B_{31}$
Ca_1	1(a)	0	0	0	$B_{11}\neq B_{22}\neq B_{33}\neq B_{23}\neq B_{31}\neq B_{12}$
Ca_2	1(b)	0	0	0.5	$B_{11}\neq B_{22}\neq B_{33}\neq B_{23}\neq B_{31}\neq B_{12}$
F_1	2(f)	$0.25+u_{F1}$	v_{F1}	w_{F1}	$B_{11}\neq B_{22}\neq B_{33}\neq B_{23}\neq B_{31}\neq B_{12}$
F_2	1(e)	u_{F2}	0.25	w_{F2}	$B_{11}\neq B_{22}\neq B_{33}\neq B_{31}$
F_2'	1(e)	$u_{F'2}$	0.25	$0.5+w_{F'2}$	$B_{11}\neq B_{22}\neq B_{33}\neq B_{31}$
F_3	2(f)	u_{F3}	v_{F3}	$0.25+w_{F3}$	$B_{11}\neq B_{22}\neq B_{33}\neq B_{23}\neq B_{31}\neq B_{12}$

Because of the weak anisotropy of the Ca and Rb surrounding, the temperature factor of these ions has been assumed isotropic and equal for each type. The results of the refinement at 4.5 K and 20 K are reported in table IV.

From this one can see that the cell parameters 2*a*, 2*b*, 2*c* are nearly equal together with a great tendancy of equality of the tilts. The observed differences are not significant. This is consistent with a tilt system $a^- a^+ a^-$ corresponding to the space group Pnma. So refinements have been redone imposing the equality of the displacements and $2a = 2b = 2c$. The Rb ion displacements have also been made to be in agreement with the Pnma space group. Table V shows the restrictions and table VI the result of the refinement at 4.5 K and 20 K. As shown in tables IV and V, when taking Pnma space group instead of $B2_1/m$ space group, the number of unknown parameters decreases from 48 to 18. The good reliability obtained with these

Table IV. — *Structural parameters of* $RbCaF_3$ *at* 20 K(*a*) *and* 4.5 K(*b*) *in the space group* $B2_1/m$.

T = 20 K 2a = 8.8692(5) 2b = 8.8724(3) 2c = 8.8687(5) β = 90.156(2)

	u	v	w	B	B_{11}	B_{22}	B_{33}	B_{23}	B_{31}	B_{12}
Rb_1	0.008(1)		0.002(1)	0.59(5)						
Rb_2	0.008(1)		0.005(1)	0.59(5)						
Ca_1				0.46(7)						
Ca_2				0.46(7)						
F_1	0.001(1)	-0.020(2)	-0.023(1)		1.03(52)	1.56(91)	1.73(52)	0.031(30)	0.87(44)	-0.18(43)
F_2	0.012(1)		-0.029(2)		-0.42(70)	1.19(67)	-0.08(51)		-0.14(38)	
F'_2	-0.019(1)		0.025(2)		1.71(55)	0.69(55)	1.29(58)		-0.77(41)	
F_3	0.021(1)	+0.024(2)	0.002(1)		0.46(36)	0.86(88)	0.01(54)	-0.26(33)	0.42(14)	-0.14(17)

R_{NUC} = 5.80 R_{PROF} = 7.19 R_{EXP} = 2.67

T = 4.5 K 2a = 8.8718(5) 2b = 8.8725(2) 2c = 8.8664(4) β = 90.157(2)

	u	v	w	B	B_{11}	B_{22}	B_{33}	B_{23}	B_{31}	B_{12}
Rb_1	0.004(1)		-0.001(1)	0.46(5)						
Rb_2	0.011(1)		0.010(1)	0.46(5)						
Ca_1				0.65(6)						
Ca_2				0.65(6)						
F_1	-0.001(1)	-0.024(1)	-0.022(1)		0.59(36)	0.15(48)	1.78(36)	-0.63(27)	-0.74(24)	0.10(26)
F_2	0.020(1)		-0.023(1)		0.61(46)	0.55(52)	1.06(61)		0.75(35)	
F'_2	-0.026(1)		0.018(1)		1.01(50)	0.11(40)	1.99(61)		-1.30(34)	
F_3	0.022(1)	0.020(2)	0.000(1)		0.56(33)	2.33(57)	0.92(29)	0.10(24)	1.21(23)	0.95(27)

R_{NUC} = 3.60 R_{PROF} = 8.22 R_{EXP} = 2.75

18 parameters allows to think that the space group of this structure is Pnma, similarly to a large majority of such perovskites [17]. The tilt angle amplitude is $\Phi = 5.01°$ at 20 K and $\Phi = 5.03°$ at 4.5 K

$$(\Phi_1 = \Phi_2 = \Phi_3 = \Phi).$$

The bond lengths (not corrected for thermal librations) are shown in figure 9 at 4.5 K. The corrected ones are plotted on figure 3.

4. **Discussion.** — 4.1 SOFT MODES. — According to Glazer's Classifications [17], in $RbCaF_3$ the successive phases correspond to the following sequence of tilts :

$$a^- a^+ a^- \overset{50K}{\rightleftharpoons} a^0 a^0 c^- \overset{193K}{\rightleftharpoons} a^0 a^0 a^0$$

$$D_{2h}^{16} \qquad D_{4h}^{18} \qquad O_h^1$$

Pnma $I\frac{4}{m}cm$ Pm3m

It is well known that the O_h^1 to D_{4h}^{18} phase transition is induced by the condensation of one of the components of the triply degenerate R_{25} mode. Assuming that the

Table V. — *Restrictions on ions displacements and anisotropic temperature factor in the cell*

$$2a \times 2b \times 2c$$

according to the tilt system $a^- a^+ a^-$ *and corresponding to the* Pnma *space group.*

	x	y	z	
Rb_1	$0.25+u_R$	0.25	$0.25+w_R$	$B_{jj} = B_R$
Rb_2	$0.25+w_R$	0.25	$0.75+u_R$	$B_{jj} = B_R$
Ca_1	0	0	0	$B_{jj} = B_{Ca}$
Ca_2	0	0	0.5	$B_{jj} = B_{Ca}$
F_1	0.25	$-u_F$	$-u_F$	$B_{22} = B_{33} = B_{1F}$ $B_{11} = B_{2F}$ $B_{23} = -B_{5F}$
F_2	u_F	0.25	$-u_F$	$B_{11} = B_{33} = B_{1F}$ $B_{22} = B_{2F}$ $B_{31} = B_{5F}$
F_2'	$-u_F$	0.25	$0.5+u_F$	$B_{11} = B_{33} = B_{1F}$ $B_{22} = B_{2F}$ $B_{31} = B_{5F}$
F_3	u_F	u_F	0.25	$B_{11} = B_{22} = B_{1F}$ $B_{33} = B_{2F}$ $B_{12} = B_{5F}$

50 K phase transition also arises out of the condensation of soft modes (in spite of the first order character of the transition [16]), it would be due to the *freezing-in* of M_3 and X_5' modes (when referring to the cubic Brillouin zone) [22]. The last one leads to rubidium displacements along | 101 |. Such a displacement can be observed in table VI.

Table VI. — *Structural parameters of* $RbCaF_3$ *at* 20 K(*a*) *and* 4.5 K(*b*) *according to the tilt system* $a^- a^+ a^-$ (Pnma *space group*).

T = 20 K	2a = 8.8701(1)	β = 90.151(2)
u_R = 0.0060(4)	w_R = 0.0065(4)	u_F = 0.0218(1)
B_R = 0.59(4) B_{Ca} = 0.46(6)	B_{1F} = 1.02(4)	B_{2F} = 0.70(5) B_{5F} = - 0.2(1)
R_{NUC} = 4.90	R_{PROF} = 8.20	R_{EXP} = 2.68

a)

T = 4.5 K	2a = 8.8705(1)	β = 90.151(2)
u_R = 0.0064(3)	w_R = 0.0061(3)	u_F = 0.0221(1)
B_R = 0.57(4) B_{Ca} = 0.62(6)	B_{1F} = 1.07(4)	B_{2F} = 0.60(5) B_{5F} = + 0.05(10)
R_{NUC} = 3.70	R_{PROF} = 9.13	R_{EXP} = 2.76

b)

4.2 PRELIMINARY REMARKS CONCERNING THE PRESENT RESULTS. — Let us first note that the temperature dependence of Ca and Rb mean square displacements displays no anomaly at the transition (fig. 5). The

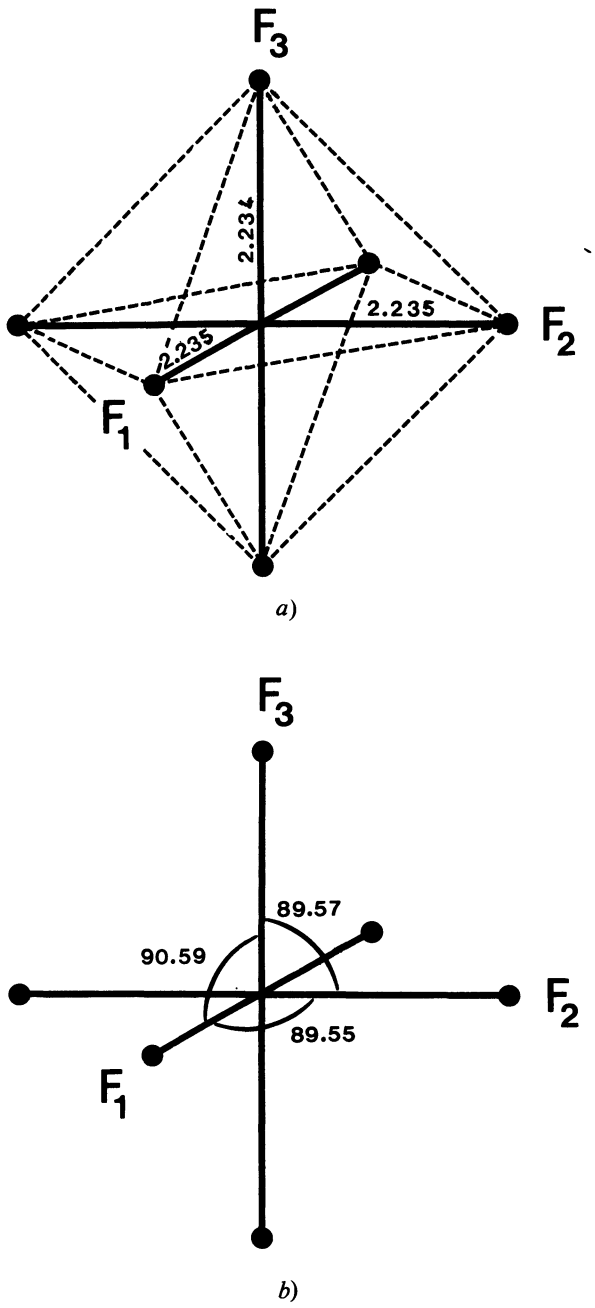

Fig. 9. — Bond lengths (Å) in the CaF_6 octahedron (*a*) and bond angles (*b*) in $RbCaF_3$ at 4.5 K.

vibrations of these ions remain isotropic within the error limit, even though this is not required by the symmetry of tetragonal phase. Such a result is reasonable because, whether or not the soft mode greatly increases the fluorine thermal motion near the transition, their polarization vector components are zero for the cations.

In the perovskite compounds it is well known that the anion octahedra are important entities and play a prominent part in phase transitions. The present results are in good agreement with the octahedra integrity. One can see that, in the tetragonal phase, $B_{11}(F_3)$ is always nearly equal to $B_{33}(F_1)$ which is

consistent with the rigidity of octahedra, and was already proved by the anisotropy of the dispersion curves [23]. In the same way, one can see in figure 3 that the CaF bond lengths $\overline{l_a}$ and $\overline{l_c}$, along | 100 | and | 001 | respectively, are nearly equal, showing the regularity of the octahedra. This regularity is also observed at the very low temperatures 20 K and 4.5 K. Another important result of this analysis is the equality and the small amplitude of the $B_{11}(F_1)$ and $B_{33}(F_3)$ factors. This can be explained by the negative value of

$$\Delta r_{CaF} = \frac{a}{2} - (r_{Ca} + r_F) = -0.057 \text{ Å [24]}$$

(r_{Ca} and r_F taken from ref. [25]) : the F^- ions are tightly wedged and so they are allowed only small displacements. This also suggests that the fluorines are pushed out of the Ca-Ca straight line and can explain their large mean square amplitude in the plane normal to this line. In spite of the fact that the soft mode R_{25} involves just such displacements, the lack of critical variation in the Debye-Waller factor due to the softening of the R_{25} mode when approaching T_c in the cubic phase seems to indicate that another phenomenon may be responsible for this large amplitude. The last point we have to discuss is that $B_{22}(F_1)$ is lower than $B_{33}(F_1)$ contrary to ref. [9] where equality of all these factors has been assumed. Our result seems to be more reasonable because $B_{22}(F_1)$ mainly depends on the R_{25} mode component which has condensed to form a c^- tilt.

The CaF_6 tilt angle in the tetragonal phase is much greater than the one deduced from the classical displacive model where $\frac{c-a}{a} = \frac{3}{2}\varphi^2$ [26] (fig. 4) which was already shown in ref. [9]. Indeed, it can be noted that the relationship $a/c = \cos\varphi$ [20] is in very good agreement with the tilt angle deduced from the refinement. This is due to the fact that the latter relation takes into account the effect of the thermal librations. A last point worth while noting is that contrary to Glazer's assumption the F_1 static displacement at the cubic to tetragonal phase transition is much weaker than its thermal motion

$$u_2(F_1) = \sqrt{u_{22}(F_1)} = \sqrt{B_{22}(F_1)/8\pi^2}\,.$$

So, the system must oscillate unsymmetrically on either side of a symmetrical configuration [20]. In fact, such a paradox can be easily explained if it is assumed an order-disorder character for this phase transition [3].

4.3 ORDER DISORDER DESCRIPTION OF THE CUBIC TO TETRAGONAL PHASE TRANSITION. — While, in the perovskite compounds family, the ferroelectric phase transitions are now well described by the order-disorder model proposed by Comes for $BaTiO_3$ [27], the antiferrodistorsive ones, related to octahedra tilts, remain an unsolved problem. The order-disorder description proposed by Rousseau [3] seems to explain many of the properties to be found near these latter ones. We are going to check this model in the light of the present results.

This model is based on the assumptions of octahedra rigid and regular, both hypotheses consistent with the present results. It is assumed that, even in the cubic phase, fluorine ions are displaced from the middle of the faces in the direction of the diagonals of these faces (fig. 10). Such displacements seem to be more

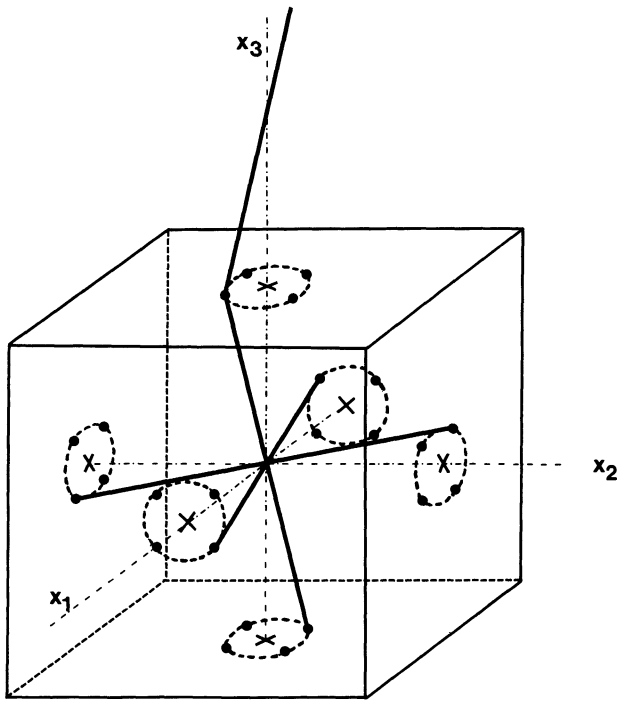

Fig. 10. — Pseudocubic cell showing the position of the wells according to the order-disorder model [3].

probable because all of the three cubic directions are equivalent contrary to what happen when anions are displaced in the direction of the bisectors of the faces.

Such a disorder is supported by the negative value of Δr_{CaF} i.e. that the Ca-Ca distance is shorter than the sum of the Ca and F diameters. So, in the high temperature phase, the cubic symmetry is due to an average effect, each of the four wells being accupied with equal probability. In the framework of this model the large thermal amplitude $B_{33}(F_1)$ and $B_{11}(F_3)$ is due to a disorder effect instead of a soft mode. The latter is hidden by the former and so, no pretransitional effect is expected for the Debye-Waller factors.

Let us turn to a quantitative study. Under the assumption of this model one can write :

$$a(T) = l(T)\cos\varphi_2(T)\cos\varphi_3(T) \quad (7)$$

$$b(T) = l(T)\cos\varphi_3(T)\cos\varphi_1(T) \quad (8)$$

$$c(T) = l(T)\cos\varphi_1(T)\cos\varphi_2(T) \quad (9)$$

where $\varphi_1\ \varphi_2\ \varphi_3$ represent the octahedra tilts about a, b, c, respectively. $l(T)$ is the CaF bond length which is assumed equal for $F_1\ F_2$ and F_3. It must be noted that under these assumptions the thermal motion is considered as normal (i.e. isotropic and small inside a well) and so it is not necessary to take it into account. In other words, at present the ordinary thermal motion is neglected.

In the cubic phase $\varphi_1 = \varphi_2 = \varphi_3$ and so $a = b = c$.

In the tetragonal phase $\varphi_1 = \varphi_2 \neq \varphi_3$ then $a = b \neq c$ and F_3 can occupy each of the four wells while for F_1 and F_2 only two wells are allowed.

The decrease of $a(T)$ with decreasing temperature results in an increase of $\varphi_3(T)$, as in the classical displacive model, while the increase of $c(T)$ is attributed to a decrease of $\varphi_1(T)$ and $\varphi_2(T)$. Assuming weak values of $\varphi_i(T)$ one can deduce for the tetragonal phase

$$\varphi_3(T) = \sqrt{1 - \frac{2\,a(T) - c(T)}{l(T)}} \qquad (10)$$

$$\varphi_2(T) = \varphi_1(T) = \sqrt{\frac{l(T) - a(T)}{l(T)}}. \qquad (11)$$

Computation of these angles needs the knowledge of $l(T)$. In the original paper of Rousseau [3] $\varphi_1(T)$ was assumed to vanish at $T = 0$ K (i.e. $l(o) = c(o)$) and the $l(T)$ temperature dependence was thought to be similar to the one of $\sqrt[3]{a^2(T)\,c(T)}$. The present study has allowed $l(T)$ computation and a good agreement with Rousseau's prediction is obtained. The difference does not lead to a discrepancy greater than $5^o/_{oo}$ in $\varphi_3(T)$ absolute value. The temperature dependence of this angle is shown in figure 4 together with the experimental and the classical displacive ones [26]. One can see the improvement brought by the order-disorder description.

In the vicinity of T_c the experimental tilt angle deviates from the order-disorder prediction (fig. 4). In fact, the system being both order-disorder (along a c axis) and displacive (in the plane perpendicular to the c axis), the discrepancy between predictions of the model and the experimental tilt angle can be seen as the contribution of the thermal motion.

In the framework of the order-disorder model, at low temperature, when thermal motions become too weak to enable fluorine jumps from a well to an other, the octahedra remain tilted about each of the $\langle\ 100\ \rangle$ axes. The experimental equality of the three tilts confirms the hypothesis of the four wells allowed for the fluorine. Otherwise, how should be possible such an equality after the large distortion undergone by the lattice in the tetragonal phase ? Furthermore, the tilt angle amplitudes (5°) are just equal to the one predicted by the order-disorder model at the cubic to tetragonal phase transition. And the first order character of the 50 K phase transition [16] is obvious when it is assumed as an order-disorder one. However it seems that the wells undergo displacements in the tetragonal phase. This behaviour indicates an abnormal character of this phase.

To the light of these results, it is not yet possible to decide wether the order-disorder description is more appropriate than the classical displacive description. In the same way, recent high resolution studies of $CsPbCl_3$ by neutron diffraction cannot display a resolvable disorder in the Cl ions [28]. However, there is now the evidence from E.P.R. experiments [29] that the probability distribution function of oxygen atoms in $SrTiO_3$ is multipeaked. The failure of diffraction techniques to come to a conclusion is probably due to their insensitivity to timescale and to the large thermal motion of atoms inside each well. Nevertheless, the equality of the tilt angles in the lowest temperature phase of $RbCaF_3$ is very promising and the study of this phase at temperatures where thermal motion must be negligeable is in progress.

Acknowledgments. — We thank the ILL for facilities.

References

[1] MULLER, K. A., in *Local properties at phase transitions*, proceeding of international school of physics ENRICO FERMI, course LIX (K. A. Muller and A. Rigamonti, North Holland) 1976.

[2] BORSA, F., in ref. [1];
BULOU, A., THEVENEAU, H., TROKINER, A. and PAPON, P., *J. Physique Lett.* **40** (1979) L-277.

[3] ROUSSEAU, M., *J. Physique Lett.* **40** (1979) L-439.

[4] RIETVELD, H. M., *J. Appl. Cryst.* **2** (1969) 65.

[5] HEWAT, A. W., *J. Phys. C* **6** (1973) 2559.

[6] CHEETHAM, A. K., TAYLOR, J. C., *J. Sol. Stat. Chem.* **21** (1977) 253.

[7] MEYER, G. M., COWLEY, R. A., *Ferroelectrics* **11** (1976) 479.

[8] HEWAT, A. W., *Phys. Status Solidi* (b) **53** (1972) K33.

[9] MAETZ, J., MULLNER, M. and JEX, H., *Phys. Status Solidi* (a) **50** (1978) K117.

[10] RIGAMONTI, A., in ref. [1].

[11] KLEEMANN, W., SCHAFER, F. J. and NOUET, J., *Physica B* (to be published).

[12] BUZARE, J. Y., FAYET, J. C., BERLINGER, W. and MULLER, K. A., *Phys. Rev. Lett.* **42** (1979) 465.

[13] MODINE, F. A., SONDER, E., UNRUH, W. P., FINCH, C. B. and WESTBROOK, R. D., *Phys. Rev. B* **10** (1974) 1623.

[14] RIDOU, C., ROUSSEAU, M., GESLAND, J. Y., NOUET, J. and ZAREMBOWITCH, A., *Ferroelectrics* (EMF., Zurich) 1975.

[15] ALMAIRAC, R., ROUSSEAU, M., GESLAND, J. Y., NOUET, J. and HENNION, B., *J. Physique* **38** (1977) 1429.

[16] HO, J. C., UNRUH, W. P., *Phys. Rev. B* **13** (1976) 447.

[17] GLAZER, A. M., *Acta. Crystallogr. A* **31** (1975) 756.

[18] HEWAT, A. W., BAILEY, I., *Nucl. Instrum. Methods* **137** (1976) 463.

[19] WILLIS, B. T. M., PRYOR, A. W., *Thermal Vibrations in Crystallography* (Cambridge University Press) 1975.

[20] GLAZER, A. M. and MEGAW, H. D., *Philos. Mag.* **25** (1972) 1119.

[21] JULLIARD, J. et NOUET, J., *Revue Phys. Appl.* **10** (1975) 325.
[22] DARLINGTON, C. N. W., *Phys. Status Solidi* (b) **76** (1979) 231.
[23] ROUSSEAU, M., NOUET, J., ALMAIRAC, R., *J. Physique* **38** (1977) 1423.
[24] NOUET, J., Thesis, Le Mans (1973).
[25] SHANNON, R. D., *Acta Crystallogr. A* **32** (1976) 751.
[26] ROUSSEAU, J. J., ROUSSEAU, M. and FAYET, J. C., *Phys. Status Solidi* (b) **73** (1976) 625.
[27] COMES, Thesis, Orsay (1969).
[28] HUTTON, J., NELMES, R. J. and MEYER, G. M. (to be published).
[29] BRUCE, A. D., MULLER, K. A. and BERLINGER, W., *Phys. Rev. Lett.* **42** (1979) 185.